Transmembrane Orientation of Hydrophobic α-Helices Is Regulated Both by the Relationship of Helix Length to Bilayer Thickness and by the Cholesterol Concentration†

Jianhua Ren, Scott Lew, Zhiwei Wang, and Erwin London*

Department of Biochemistry and Cell Biology and the Department of Chemistry, State University of New York at Stony Brook, Stony Brook, New York 11794-5215

Received April 22, 1997; Revised Manuscript Received June 18, 1997⊗

ABSTRACT: A fluorescence-based approach to evaluate the regulation of transmembrane orientation of α-helices has been developed to examine the behavior of a membrane-inserted α-helical peptide with a 19 residue hydrophobic sequence. The emission λ_{max} of a Trp residue in the helix was used to determine its location in the bilayer. To calibrate this method, Trp λ_{max} and depth (determined by parallax analysis of fluorescence quenching) were measured for transmembrane peptides with Trp at different positions. Transmembrane orientation of the α-helix was found to be destabilized by differences between the width of the bilayer and the length of the hydrophobic sequence (i.e., hydrophobic mismatch). When bilayer width exceeded the length of the hydrophobic segment, mismatch induced formation of a nontransmembraneous orientation close to the polar/hydrocarbon interface. By manipulation of bilayer width *in situ*, it was found that the transmembrane and nontransmembrane orientations could interconvert. Cholesterol altered the transmembrane/nontransmembrane equilibrium to a degree consistent with its tendency to increase bilayer thickness. Evaluation of the energetics of transmembrane vs nontransmembrane insertion showed increased mismatch of a helix with bilayer width by the equivalent of just one hydrophobic residue can destabilize transmembrane orientation by roughly 0.5 kcal/mol. Inclusion of 30 mol % cholesterol in a bilayer can alter transmembrane insertion stability by 3−5 kcal/mol. Thus, physiologically relevant variations in both the hydrophobic helix length/membrane thickness ratio and the cholesterol levels influence transmembrane insertion significantly.

Transmembrane sequences that contact lipid must be long enough to span the hydrophobic core of the bilayer. The mismatch between bilayer width and hydrophobic sequence length has been found to strain both the lipid bilayer (Nezil & Bloom, 1992; Zhang et al. 1992b; Killian et al., 1996) and membrane protein structure (Caffrey & Feigenson, 1981; Johannsson et al., 1981). One of the physiological factors that controls bilayer thickness is cholesterol content (Nezil & Bloom, 1992). It has been proposed that the cholesterol content of a membrane plays a central role in the localization of membrane proteins to different organelles via cholesterol effects on bilayer width (Bretscher & Munro, 1993). This proposal is supported by the observation that the hydrophobic sequence length of transmembrane proteins residing in different organelles correlates with cholesterol level (Bretscher & Munro, 1993; Munro, 1995). Nevertheless, the consequences of helix length and cholesterol content both on helix structure and orientation have not yet been determined.

In this report, a new approach is introduced to measure the energetics of transmembrane orientation of α-helices. Lys-flanked poly Leu (pLeu) peptides have been shown to form transmembrane helices (Davis et al., 1983; Huschilt et al., 1989; Zhang et al., 1992a), and it has been shown that introduction of a Trp at the center of the Leu stretch does not perturb their transmembrane structure (Bolen & Holloway, 1990). It is demonstrated here that by monitoring the depth of the Trp residue using fluorescence emission λ_{max} and the parallax analysis fluorescence quenching method (Chattopadhyay & London, 1987; Abrams & London, 1993), the location of the helix in the membrane can be measured. This allows evaluation of the equilibrium between transmembrane and nontransmembrane orientations. It is found that both the ratio of helix length to the bilayer width and cholesterol content have a marked effect on the behavior of membrane-inserted α-helices under physiologically relevant conditions.

EXPERIMENTAL PROCEDURES

Materials. The peptides $K_2GL_7DLWL_9K_2A$ [pLeu(D11)], $K_2WL_9AL_9K_2A$, $K_2CLWL_7AL_9K_2A$, $K_2CL_3WL_5AL_9K_2A$, $K_2CL_5WL_3AL_9K_2A$, $K_2CL_7WLAL_9K_2A$, and $K_2CL_9WL_9K_2A$ were purchased from Research Genetics, Inc. (Huntsville, AL). The peptides all had acetylated N-termini and amide-blocked C-termini. Phosphatidylcholines (PCs, 1,2-diacyl-*sn*-glycero-3-phosphocholines), di C14:1Δ9c PC (dimyristoleoyl PC), di 16:1Δ9c PC (dipalmitoleoyl PC); di 18:1Δ9c PC (dioleoyl PC); di 20:1Δllc PC (dieicosenoyl PC); di 22:1Δ13c PC (dierucoyl PC); di 24:1Δ15c PC (dinervonoyl PC); 5 or 12 SLPC, 1-palmitoyl-2-(5- or 12 doxyl)stearoyl PC; and TempoPC, [1,2-dioleoyl-*sn*-glycero-3-(4-(*N*,*N*-dimethyl-*N*-(2-hydroxyethyl)ammonium)-2,2,6,6-tetramethylpiperidine-1-oxyl] were purchased from Avanti Polar Lipids, Inc. (Alabaster, AL). Cholesterol and decane were from Aldrich (St. Louis, MO). Lipid purity was assessed by TLC as previously described (Abrams & London, 1993). No significant impurities were observed with loadings that were generally over 20 μg.

† This work was supported by NIH Grant R01 GM 48596.
⊗ Abstract published in *Advance ACS Abstracts,* August 1, 1997.

S0006-2960(97)00929-X CCC: $14.00

Peptides were purified on a Rainin Dynamax HPLC equipped with a reverse phase C18 column. Mobile phase mixtures of 0.5% TFA/isopropyl alcohol and 0.5%TFA/H_2O were used to elute peptides using shallow isopropanol gradients at a flow rate of 0.4 mL/min (Lew & London, 1997). Elution of the purified peptides generally occurred between 50 and 70% isopropyl alcohol. The pH value of peptide elute was adjusted to near neutral (with NaOH) and stored at −20 °C. The purity of the peptides was confirmed with MALDI-TOF mass spectrometry (Center for the Analysis and Sequence of Macromolecules, SUNY, Stony Brook) using α-cyanohydroxycinnamic acid as the matrix and bovine insulin as a molecular weight standard. Peptides examined on MALDI-TOF generally appeared to be >95% pure. Some of the Cys containing peptides contained a significant proportion of dimers, presumably linked via disulfide bonds. Peptide concentration was determined from the UV absorbance at 280 nm by using $\epsilon = 5\ 500\ M^{-1}\ cm^{-1}$.

Sample Preparation. Mixtures of lipids, cholesterol, and peptides were dried first under nitrogen and then 1 h at high vacuum. For ethanol dilution vesicles, 10 μL of 100% ethanol was added to dissolve the samples. Then, 600 μL of 12 mM mixed Na and K phosphate, 137 mM NaCl, 3 mM KCl, pH 7.4 (PBS) (Sambrook et al., 1989) was added and vortexed to disperse the lipid/peptide mixture mainly in the form of small unilamellar vesicles (SUV) (Batzri & Korn, 1973). Final phospholipid concentration was 200 μM, and peptide concentration was 2.5 μM. For crude multilamellar vesicles (MLV), the dried lipids were hydrated directly in PBS. For freeze−thaw large unilamellar vesicles, a preparation of MLV was sonicated for 20 min in a bath sonicator (Lab Supplies, Hicksville, NY) and then freeze−thawed on dry ice/acetone 4−5 times. For 1000 Å diameter extrusion vesicles, a preparation of freeze−thaw vesicles was passed 21 times through a microextruder (Avestein, Ottawa, Canada) equipped with a 1000 Å polycarbonate filter (Hope et al., 1985). (In control experiments, the effect of adding 10 μL ethanol to vesicles prepared by each method was examined. No effect on Trp λ_{max} was found.)

Circular Dichroism Measurements. Circular dichroism (CD) spectra were recorded using a JASCO J-715 CD spectrometer using 1 mm quartz cuvettes at room temperature. Typically, final spectra were the average of 40 scans taken at 50 nm/min. Estimation of α-helical content was done using the SELCON program (Sreerama & Woody 1993, 1994). Background spectra (lipids plus buffer) were subtracted before analysis of secondary structure.

Fluorescence Measurements. Tryptophan fluorescence was measured on a SPEX τ2 Fluorolog spectrofluorometer operating in the steady state mode. Emission spectra were measured in a semimicro quartz cuvette (1 cm excitation pathlength and 4 mm emission pathlength) with excitation at 280 nm, generally using a 2.5 mm excitation slit and 5 mm emission slit. The fluorescence of background samples without peptide was measured and subtracted from reported data. In the decane addition experiments, fluorescence was measured 5 min after addition of 5 μL aliquots of 1/9 (v/v) decane/ethanol to the peptide-containing SUV. This was sufficient to allow equilibration of decane into the bilayers as judged by the stabilization of Trp fluorescence. Samples were measured at room temperature unless otherwise noted. For measurements at specific temperatures (16, 23, or 33 °C) the samples were placed in a temperature controlled sample holder.

Samples for Parallax Analysis Measurement. For parallax analysis experiments, vesicles made by dilution from ethanol were prepared containing di C18:1 PC and 15% quencher-(nitroxide)-labeled lipid (either TempoPC, 5 SLPC, or 12SLPC) as previously described (Abrams & London, 1993). Duplicate samples were prepared as above except that after drying they were dissolved with 20 μL of ethanol and dispersed with then 980 μL of 10 mM Na phosphate, 150 mM NaCl, pH 7.5−7.6. Final peptide concentration was 2 μM and lipid concentration 200 μM. Emission intensity was recorded at the wavelength of maximum emission at room temperature.

THEORY

Calculation of Depth. Parallax analysis has been discussed in detail in previous publications (Chattopadhyay & London, 1987; Abrams & London, 1992, 1993). The distance of Trp residues from the bilayer center (z_{cf}) was calculated from the parallax equation:

$$z_{cf} = L_{c1} + [(-1/\pi C(\ln(F_1/F_2)) - L_{21}^2)/2L_{21}]$$

where L_{c1} is the difference in depth between the shallow quencher and the bilayer center, F_1 and F_2 are the fluorescence intensities in the presence of the shallow and deeper quencher, respectively, L_{21} is the difference in depth between the shallow and deeper quencher, and C is the concentration of quencher in molecules/Å^2 (Chattopadhyay & London, 1987).

Calculating the Depth of Deep Fluorophores from the Parallax Analysis. The standard parallax analysis is appropriate when a fluorophore is only quenched by nitroxide-labeled lipids that are in the same leaflet of the bilayer as the fluorophore. When a fluorophore is deeply buried, it can be quenched by deep nitroxides in the other (trans) leaflet of the bilayer. We previously derived an expression to analyze such cases (Chattopadhyay & London, 1987), but the expression was for cases where the *lateral* approach of fluorophore to the quencher in the trans leaflet is not restricted. We have now derived an expression for cases in which the lateral approach of quenchers to fluorophore is the same in both leaflets as in the case of a transmembrane helix. To do this, we start with the expressions for quenching of a fluorophore deep enough in the bilayer such that it can be quenched by the deep quencher 12SLPC in both leaflets, but only by the shallower quencher 5SLPC in the same leaflet as the fluorophore. In this case for the 5SLPC, quenching will be given by (Chattopadhyay & London, 1987):

$$F_1/F_o = \exp(-\pi R_c^2 C + \pi z_{1f}^2 C + \pi x^2 C)$$

where F_o is the fluorescence intensity in the absence of quencher, R_c is the critical quenching distance [apparent maximum distance between quencher and fluorophore giving quenching (Chattopadhyay & London, 1987)], z_{1f} is the difference in depth between 5SLPC and the fluorophore; and x is the minimum allowed lateral distance between fluorophore and quencher. For 12SLPC,

$$F_2/F_o = \exp(-\pi {R_c}^2 C + \pi {z_{2f}}^2 C + \pi x^2 C) \times \exp(-\pi {R_c}^2 C + \pi {z_{t2f}}^2 C + \pi x^2 C)$$

where z_{2f} is the difference in depth between the fluorophore and 12SLPC in the same leaflet of the bilayer as the fluorophore and z_{t2f} is the difference in depth between the fluorophore and the 12 SLPC in the opposite (trans) leaflet of the bilayer. Making the substitutions $z_{1f} = z_{2f} - L_{21}$ and $z_{t2f} = 2L_{c2} + z_{2f}$ (where L_{c2} is the difference in depth between the 12SLPC and the bilayer center), taking the natural log of both equations, multiplying ln(eq 2) by 2, and subtracting eq 3 from 2 gives

$$2\ln(F_1/F_o) - \ln(F_2/F_o) = 2\pi(z_{2f} - L_{21})^2 C - \pi {z_{2f}}^2 C - \pi(2L_{c2} + z_{2f})^2 C$$

Rearrangement and substitution of $z_{cf} = z_{2f} + L_{c2}$ gives

$$z_{cf} = L_{c2} - [(1/\pi C(\ln((F_1/F_0)^2/(F_2/F_0))) - 2{L_{21}}^2 + 4{L_{c2}}^2)/4(L_{21} + L_{c2})]$$

Equation 4 was used for the deeper Trp residues (identified by those giving $z_{cf} < 5$ Å when depth was calculated from eq 1).

Evaluation of the Energetics of Transmembrane Orientation. The amount of each fluorescence species present in a binary mixture can be determined from λ_{max} when the species have similar intensities and slightly different λ_{max} values. To a first approximation for a mixture of transmembrane (TM) and nontransmembrane (nonTM) helices, fraction TM helix $= (\lambda_{max\ nonTM} - \lambda_{max})/(\lambda_{max\ nonTM} - \lambda_{max\ TM})$, and fraction nonTM helix $= 1 -$ fraction TM helix. Estimated values for $\lambda_{max\ TM}$ and $\lambda_{max\ nonTM}$ were 317.5 and 331 nm, respectively, for pLeu(D11) (see Results).

This information allows calculation of the transmembrane orientation equilibrium constant (K_{TM}) and free energy: K_{TM} = (fraction TM helix)/(fraction nonTM helix); $\Delta G_{TM}° = -RT \ln K_{TM}$, respectively. The difference in transmembrane orientation energies in any two samples (e.g., 1 and 2) is $\Delta\Delta G_{TM}° = -RT \ln K_{TM1} + RT \ln K_{TM2} = -RT \ln (K_{TM1}/K_{TM2})$. Notice that the lowest energy nontransmembrane state is not necessarily the solution state of the helix.

RESULTS

Membrane Location of the Hydrophobic Peptide pLeu-(D11) Is Affected by Bilayer Width. The pLeu peptides have long Leu sequences flanked by Lys residues. They have been found to take on a transmembrane helical structure in ordinary bilayers (see Introduction). In order to see how transmembrane insertion is affected by bilayer width, the behavior of a pLeu peptide was investigated in a series of bilayers with different acyl chain lengths. [Previous studies have shown that the width of the hydrophobic region of the bilayer is almost linearly dependent on acyl chain length (Caffrey & Feigenson, 1981; Lewis & Engelman, 1983)]. The peptide chosen, pLeu(D11), has a hydrophobic sequence (19 residues) close in length to that typical for many proteins with single transmembrane sequences (Landolt-Marticorena et al., 1993). This hydrophobic sequence also has a single deep Asp residue and a central Trp residue which allows its behavior to be monitored by fluorescence.

Figure 1A shows the effect of acyl chain length on the emission maximum of the Trp residue in pLeu(D11). Emission is most blue shifted in di C18:1 PC and di C20:1 PC. There is a progressive shift in Trp emission to longer wavelengths both in bilayers with shorter or longer acyl chain lengths. This effect does not appear to be dependent on the exact details of acyl chain structure, because a similar result is obtained with mixtures of the shortest and longest acyl chain lipids (Figure 1B). Because Trp emission is more red shifted in a more polar environment, the wavelength shifts suggest some sort of change in which pLeu(D11) is most deeply inserted in di C 18:1 PC and at extremes of bilayer width moves to a shallower location (see below).

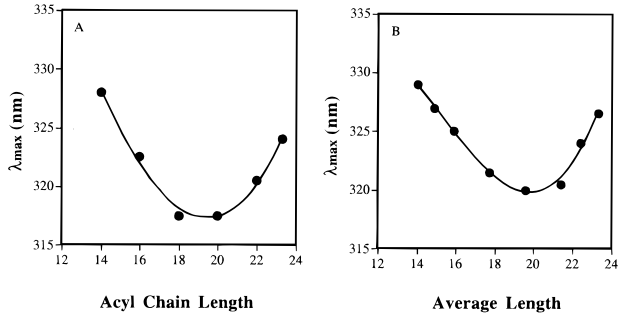

FIGURE 1: Effect of acyl chain length on Trp emission of model membrane incorporated pLeu(D11). (A) pLeu(D11) inserted into model membrane vesicles with a uniform acyl chain length. (The exception was that for the longest acyl chains a 2/1 mol/mol di C24:1 PC/di C22:1 PC was used so that the bilayer would remain in the fluid state). The T_m of pure di C24:1 PC is close to room temperature (Caffrey & Feigenson, 1981). (B) pLeu(D11) inserted into model membrane vesicles formed by various mixtures of thin and thick acyl chain lengths. Samples contained 0, 10, 20, 40, 60, 80, 90, and 100 mol % of di C14:1 PC mixed with 2/1 di 24:1 PC/di C22:1 PC. The average length was calculated from the percent composition of each lipid.

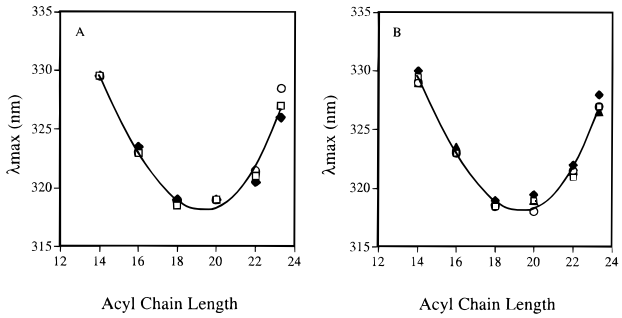

FIGURE 2: Effect of temperature and model membrane type on the Trp emission of pLeu(D11) incorporated in model membrane vesicles. (A) Effect of temperature. (○) 16 °C; (□) 23 °C; (◆) 33 °C. (B) Effect of model membrane type. (□) ethanol dilution vesicles; (◆) crude multilamellar vesicles; (○) freeze−thaw large unilamellar vesicles; (▲) 1000 Å diameter vesicles formed by extrusion.

The effect of temperature and the manner of vesicle preparation was examined to see if these factors would affect the acyl chain length dependence of the Trp emission maximum. As shown in Figure 2, Trp emission properties were not strongly influenced by either of these factors.

pLeu(D11) Location Can Be Regulated by Changing Bilayer Width in situ: Different Forms of pLeu(D11) Are in Dynamic Equilibrium. The addition of decane, which becomes incorporated at the bilayer center, is another method to alter bilayer width (Haydon et al., 1977; Johannsson et al., 1981). Studies on the effect of membrane thickness on the activity of the transmembrane Ca^{2+}ATPase protein have

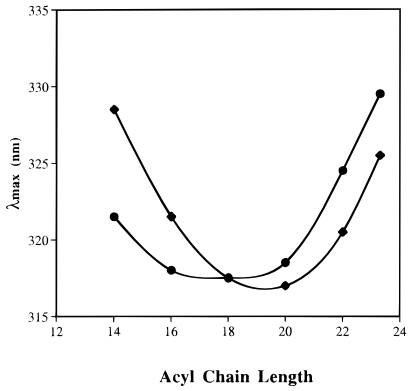

FIGURE 3: Effect of decane on emission λ_{max} of pLeu(D11) incorporated into model membrane vesicles with different acyl chain lengths. Lipids used were the same as in Figure 1A. (●) λ_{max} without decane. (◆) λ_{max} after addition of 5 μL 1:9 (v/v) decane/ethanol. Ethanol alone has no effect on λ_{max}.

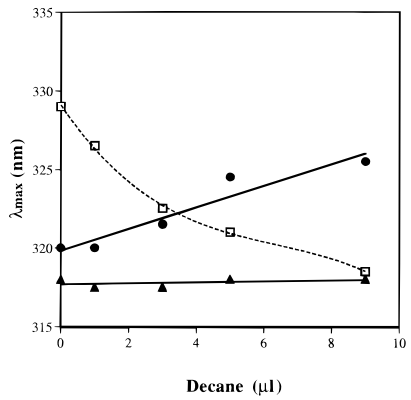

FIGURE 4: Effect of decane concentration on emission λ_{max} of pLeu-(D11) incorporated into model membrane vesicles with different acyl chain lengths. (□) di C14:1 PC; (▲) di C18:1 PC; (●) di C22:1 PC. Fluorescence was measured 5 min after aliquots of 1:9 (v/v) decane/ethanol were added. Values stabilized within 3 min.

shown decane addition has very similar effects on activity as does variation of membrane thickness by altering acyl chain length (Johannsson et al., 1981). Decane addition was used to examine whether the effect of bilayer width on pLeu-(D11) would be independent of the method used to alter bilayer width. In addition, decane addition was used because it allowed regulation of membrane width *in situ*.

Figures 3 and 4 show the effect of addition of decane on Trp emission in bilayers with various acyl chain lengths. In thin bilayers, addition of decane appears to increase Trp depth (i.e., Trp emission shifts to shorter wavelengths). In contrast, for thick bilayers, decane addition decreases Trp depth. These are the changes predicted for the increase in bilayer width upon decane addition. Overall, the acyl chain length at which Trp emission is at the shortest wavelengths, i.e., in which pLeu(D11) is deepest, is shorter in the presence of decane, again as is predicted for a decane-induced increase in bilayer width (Figure 3). It should also be noted that pLeu(D11) remains deeply located in di C18:1 PC both in the absence and presence of decane.

The effect of decane is also interesting because it demonstrates pLeu(D11) location can be altered *in situ*. Since the shift in emission wavelength induced by decane stabilized within a couple of minutes, it appears decane incorporation into the bilayer and the change in peptide location are relatively rapid events. Finally, it should be noted that the effect of decane is dose dependent (Figure 4), as is expected

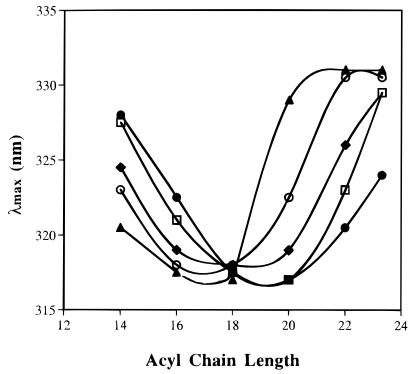

FIGURE 5: Effect of cholesterol on emission λ_{max} of pLeu(D11) incorporated into model membrane vesicles with different acyl chain lengths. Phospholipids used were the same as in Figure 1A. λ_{max} (●) without cholesterol; with (□) 5 mol % cholesterol; (◆) 10 mol % cholesterol; (○) 20 mol % cholesterol; (▲) 30 mol % cholesterol.

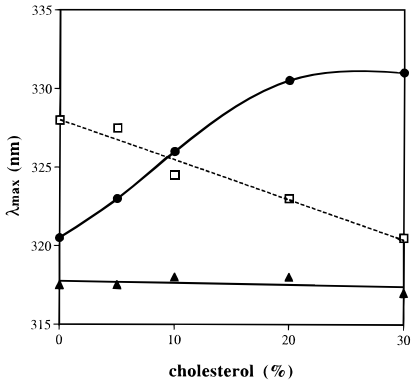

FIGURE 6: Effect of cholesterol concentration on emission λ_{max} of pLeu(D11) incorporated into model membrane vesicles with different acyl chain lengths. Samples contained mixtures of cholesterol and (□) C14:1 PC; (▲) Di C18:1 PC; (●) di C22:1 PC.

since the bilayer becomes progressively thicker as more decane is added (Haydon et al., 1977).

Importantly, these experiments demonstrate that the different pLeu(D11) states are in dynamic equilibrium with each other, rather than trapped in one or the other location. This is important because it allows analysis of energetics of the conformational change (see below).

Cholesterol Regulates Location of pLeu(D11). It has been proposed that cholesterol level controls transmembrane protein behavior by increasing bilayer width (Bretscher & Munro, 1993). Therefore, the effect of cholesterol on pLeu-(D11) behavior was also examined.

Figure 5 shows the effect of cholesterol on the emission maximum. In general, the effects of cholesterol addition are very similar to those of decane. For example, as in the case of decane, for thin bilayers, addition of cholesterol appears to increase Trp depth (i.e., Trp emission shifts to shorter wavelengths), and for thick bilayers, cholesterol addition decreases Trp depth. Both Figure 5 and 6 show pLeu(D11) depth in di C18:1 PC is insensitive to the addition of cholesterol.

Figure 6 shows that there is a smooth dependence of the wavelength shifts on cholesterol concentration, and it is noteworthy that even small changes in overall cholesterol (by 5% of total lipid) can have significant effects.

The Nature of the Conformational Change at Extremes of Bilayer Width: Membrane Width Does Not Significantly Affect Secondary Structure of pLeu(D11). To see if the changes in pLeu(D11) behavior were linked to a change in

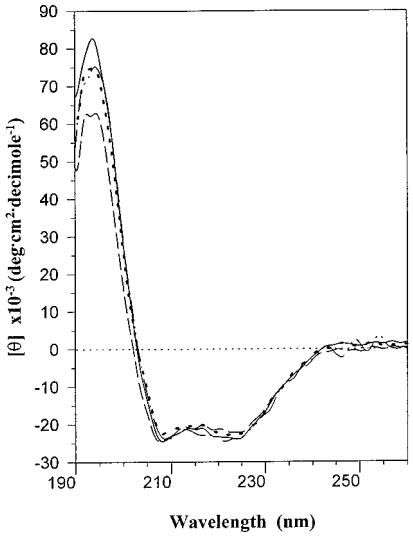

FIGURE 7: CD spectra of pLeu(D11) in model membrane vesicles. (•••) pLeu(D11) incorporated in di C18:1 PC vesicles (analysis of which gives 76% α-helix); (—) incorporated in 2/1 mol/mol di C24:1 PC/di C22:1 PC vesicles (78% α-helix); (- •• -) incorporated in 2/1 mol/mol di C24:1 PC/di C22:1 PC vesicles containing 5% cholesterol (73% α-helix); (- - - - -) incorporated in di C14:1 PC vesicles (72% α-helix). In each case, lipid plus buffer backgrounds have been subtracted from spectra shown.

secondary structure, circular dichroism (CD) of pLeu(D11) incorporated in model membranes was measured. As shown in Figure 7, membrane-inserted pLeu(D11) gave a characteristic α-helix CD signal. Using a standard analysis program (Sreerama & Woody, 1993, 1994), α-helix content was about 75%, in agreement with previous studies showing that pLeu peptides are largely α-helical (Zhang et al., 1992a). This fraction of α-helix (19 out of 25 residues) corresponds to the fraction of the peptide in the hydrophobic stretch, and it appears that residues outside the hydrophobic core of the peptide largely nonhelical (Zhang et al., 1992a).

Analysis of Figure 7 also showed that the secondary structure of pLeu(D11) does not change significantly when membrane thickness was varied.[1] This means that the changes in Trp emission seen at various bilayer widths are not due to changes in secondary structure. Similar results have been noted for other pLeu peptides (Zhang et al., 1992b).

It should be noted that pLeu(D11) dissolved directly into aqueous solution gave a much weaker CD signal than in any of the samples containing model membranes (not shown). This result indicates that the change in Trp emission with membrane thickness does not reflect dissociation of the peptide from the bilayer (also see below).

Nature of the Conformational Change at Extremes of Bilayer Width: Calibrating the Relationship between Trp Depth and Emission Wavelength. Since secondary structure is not altered by bilayer width, the most likely explanation of the Trp fluorescence emission changes is that they simply reflect a change in helix location in the membrane. In order to evaluate this change, Trp depth within the bilayer had to be pinpointed.

[1] Interestingly, the small decrease seen in signal intensity at 195 nm in the di C14:1 PC bilayers relative to the other model membranes could be reversed by addition of decane, suggesting it reflects some characteristic associated with bilayer width.

Table 1: Distance of Trp from the Bilayer Center in di C18:1 PC Vesicles for Various pLeu Helices Calculated by Parallax Analysis and Trp Emission Spectrum Width[a]

peptide	$F_{[+Quencher]}/F_{[-Quencher]}$ (F/F_o) tempo PC	5SLPC	12SLPC	z_{cf} (Å)	$W_{1/2}$ (nm)[b]
$K_2WL_9AL_9K_2A$	0.38	0.32	0.41	14.3[c]	59
$K_2CLWL_7AL_9K_2A$	0.45	0.325	0.335	9.4	59
$K_2CL_3WL_5AL_9K_2A$[d]	0.36	0.32	0.265	6.9	58
$K_2CL_5WL_3AL_9K_2A$	0.50	0.355	0.16	5.4	59
$K_2CL_7WLAL_9K_2A$	0.70	0.56	0.105	1.3	57
$K_2CL_9WL_9K_2A$	0.50	0.59	0.041	−1.8	54
$K_2GL_7DLWL_9K_2A$	0.56	0.42	0.073	2.0	56

[a] Samples with quencher contained di C18:1 PC with 15 mol % nitroxide-labeled lipid. Calculation of z_{cf} was performed using the strongest quenching of either the 5SLPC/12SLPC or 5SLPC/TempoPC pair (Abrams & London, 1993). For details see Experimental Procedures. The results shown are the average of duplicate or more samples. For the Asp peptide, two experiments with duplicates were performed and gave very similar z_{cf} values. [b] $W_{1/2}$ is the width of the Trp emission spectra at half-maximal intensity. [c] Quenching by 12SLPC is close enough to that by TempoPC in this case so that the average of depth of using 5SLPC/12SLPC or 5SLPC/TempoPC pairs may be more accurate than just the latter pair alone (Abrams & London, 1993). This average gives a $z_{cf} = 13$ Å. [d] This peptide contained a large amount of a peptide with a two residue deletion. This contaminant was unresolved on HPLC.

To do this we evaluated the relationship between Trp emission and Trp depth. Trp emission maximum was measured for a series of pLeu peptides in which the position of a single Trp residue was varied. To confirm that the Trp in these pLeu peptides were really at different depths, Trp location was measured directly by fluorescence quenching using parallax analysis. In this method, the depth of a fluorophore is calculated from the ratio of its quenching by lipids carrying a nitroxide (spin) label at different depths (Chattopadhyay & London, 1987; Abrams & London, 1993). We have previously shown that the parallax analysis gives accurate depths in a wide variety of cases (Abrams & London, 1992, 1993; Asuncion-Punzalan & London, 1995; Kachel et al., 1995). Table 1 shows the correlation between quenching and Trp position in the helix. z_{cf}, the calculated distance of the Trp from the bilayer center is also shown. As expected for a transmembrane structure, depth increases as the Trp is moved to positions progressively farther from the polar N-terminus of the peptide. A Trp at the center of the Leu stretch was the deepest in the bilayer. Comparison of z_{cf} with Trp position gave an average slope of 1.5 Å change in depth per residue change in position (Figure 8A). This is exactly as expected for a transmembrane α-helix. The actual Trp depths are close to those predicted for a transmembrane α-helix, but on the average 1.7 Å deeper than that predicted for the depth of the Trp attachment site on the helix backbone. We are not certain whether this small difference between measured Trp depth and that predicted for their attachment site largely reflects actual Trp locations or experimental limitations, such a perturbation of quencher location by the peptide. In any case, the Trp series of pLeu peptides clearly forms the expected transmembrane α-helices, with the Trp at different depths. The close correspondence of the depth values to those predicted for a transmembrane helix illustrates the basic accuracy of the parallax analysis approach.

On the basis of this information, Trp emission properties can be evaluated as a function of membrane depth. As shown in Figure 8B, there is a progressive red shift in

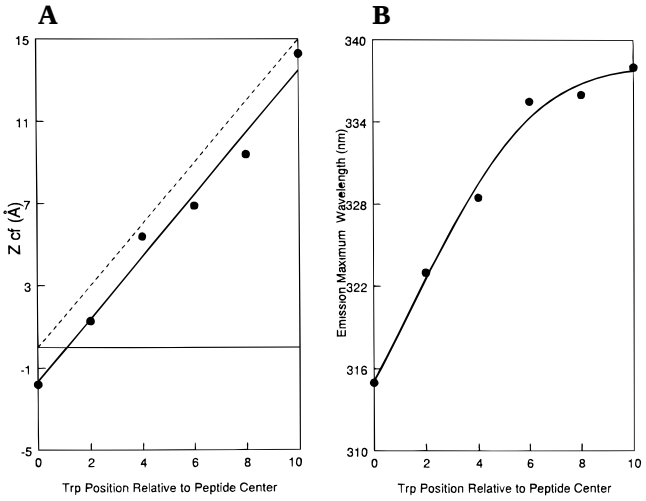

FIGURE 8: Effect of Trp sequence position in pLeu helices on Trp location in the bilayer and fluorescence emission λ_{max}. (A) (Left) Effect of Trp position on depth. z_{cf} (from Table 1) vs Trp position relative to peptide center (defining the central residue in the peptide as position 0). (Solid line) Linear least-squares fit to z_{cf}. (Dashed line) Predicted z_{cf} for the Trp attachment site on the helix backbone assuming an untilted helical structure. (B) (Right) Effect of Trp position on emission λ_{max} for model membrane incorporated pLeu peptides. The λ_{max} of peptides $K_2WL_9AL_9K_2A$, $K_2CLWL_7AL_9K_2A$, $K_2CL_3WL_5AL_9K_2A$, $K_2CL_5WL_3AL_9K_2A$, $K_2CL_7WLAL_9K_2A$, and $K_2CL_9WL_9K_2A$ was measured in di C18:1 PC vesicles.

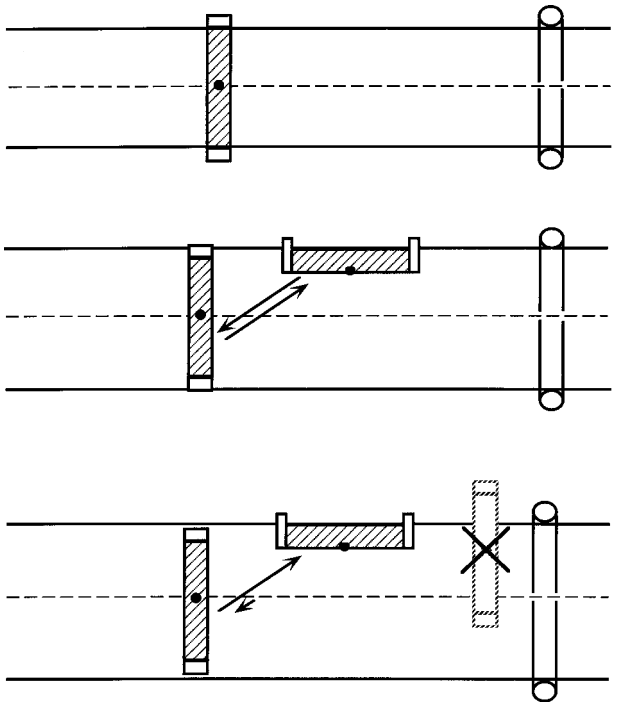

FIGURE 9: Schematic diagram of pLeu(D11) orientation in bilayers with different thickness. (●) indicates the location of the central Trp residue. The hydrophobic section of the peptide is shown as hatched. The polar ends are shown unfilled. (Top) Likely orientation in di C18:1 PC. (Middle) Likely orientation in slightly thicker membranes. (Bottom) Likely orientation in thickest membranes. See text for details.

emission λ_{max} as Trp position is moved closer to the end of the peptide (and thus closer to the bilayer surface). This change is not linear, being more sensitive to depth close to the bilayer center. These values may be generally useful for evaluating the location of Trp in membrane inserted peptides and proteins.[2]

Spectral width also contains information about location. The Trp emission spectra are narrowest for Trp near the center of the bilayer. This is consistent with Trp location, as solvent induced broadening is generally more severe in polar environments (Cantor & Schimmel, 1980).

Nature of the Conformational Change at Extremes of Bilayer Width: pLeu(D11) Switches from Transmembrane to Nontransmembrane Orientations. Using the information above, Trp emission wavelength could be used to evaluate the location of pLeu(D11) in the membrane. Comparison to Figure 8 shows that the value of 318−320 nm seen in di C18:1 PC corresponds to a Trp location close to the center of the bilayer. This was confirmed by parallax analysis measurements (Table 1)[3] and corresponds to a predominantly transmembrane structure for this helix (Figure 9, top).

The large red shift in very thick bilayers corresponds to a change in Trp location. By comparison to Figure 8 and Table 1, the limiting value of λ_{max} observed for pLeu(D11) (331 nm), would correspond to a Trp location roughly 7 Å from the bilayer center in di C18:1 PC.

With what α-helical conformations is this change in Trp location consistent? In the thickest bilayers the shallower Trp location is *inconsistent* with a partially transmembrane conformation, because it would require that the Lys residues become deeply buried in the hydrophobic bilayer core (Figure 9, bottom). For the same reason, a model in which the peptide is unanchored and floats freely within the hydrophobic core of the bilayer can be ruled out. A much more likely model comes from the fact that the λ_{max} of 331 nm is similar to that previously reported for Trp on the nonpolar face of a membrane-penetrating amphipathic helix oriented parallel to the membrane surface (Chung et al., 1992). Thus, it is likely that in the thickest bilayers the pLeu helix predominantly has a nontransmembraneous orientation relatively parallel to (but perhaps somewhat below) the membrane surface, such that the Trp is on the face of the helix closest to the bilayer center and the more polar Asp (which is on the face of the helix opposite the Trp) at a much shallower location on the side of the helix closest to the aqueous solution.

This conclusion is supported by preliminary results with helices having shorter hydrophobic sequences than pLeu-(D11). Parallax analysis indicates a shallower location in di C18:0 PC when the hydrophobic region is shortened (data not shown).

In a bilayer with a hydrophobic core that is slightly thicker than that of the peptide, there was an intermediate λ_{max}, suggesting an equilibrium between coexisting transmembrane and nontransmembrane forms (Figure 9, middle). (Again, the alternative of a conformation with one polar end buried within the bilayer, although not as deeply as in the thickest

[2] Investigators wishing to use these values should adjust for instrumental differences. To help do so, it should be noted that indole λ_{max} on our instrument was 333 nm in ethanol and 351 nm in water. We would also caution that the Trp λ_{max} values are only appropriate for Trp residues in contact with the bilayer. A Trp buried within a protein would have a λ_{max} influenced by its interaction with other residues.

[3] The quenching of pLeu(D11) by 15 mol % 12SLPC was also measured in the 2/1 di C24:1 PC/di C22:1PC mixture, and in di C14:1 PC. In these cases quenching was about 90%. Since quenching is incomplete even when a fluorescent group is totally membrane bound, this result confirms that the pLeu peptides are fully membrane associated even at the extremes of bilayer width.

bilayers, is unlikely.) The width of the Trp emission spectra under different conditions supports the conclusion that two forms coexist. If two forms with different λ_{max}s are present in one sample, then the width of the emission spectrum should increase. This is seen for pLeu(D11) in samples where λ_{max} has an intermediate value between the transmembrane (315−318 nm) and nontransmembrane (331 nm) forms. For example, pLeu(D11) in di C 22:1 PC (λ_{max} = 321) has a spectral width of 62 nm, and in 2/1 di C 24:1/di C 22:1 PC mix (λ_{max} = 325−327) has a spectral width of 63 nm. These values are larger than those (54−59 nm) for peptides with a fixed Trp depth (Table 1). Inclusion of 20% cholesterol with the di C24:1 PC/di C22:1 PC mix, which fully shifts the pLeu(D11) peptide into the nontransmembrane conformation (λ_{max} 331, Figure 5), resulted in a narrowing of the emission spectrum to 59 nm, as would be predicted.

The change in λ_{max} in thin (di C14:1 PC) membranes may or may not reflect a conformation that is nontransmembraneous. Some or all of the λ_{max} shift in thin bilayers relative to di C18:0 PC may be due to the fact that in a thinner membrane even a Trp at the center of the bilayer is automatically closer to the surface. Of the possible structures in a thin bilayer, a transmembrane structure protruding from the bilayer is very unlikely as it would expose Leu residues to aqueous solution. A bent structure (e.g., part of the peptide transmembraneous and part parallel to the bilayer surface) is possible, but would predict a loss of α-helix structure for several residues, and no change in α-helix or turn content was detected in the analysis of CD spectra. The most likely transmembrane structure would be transmembraneous but highly tilted. There is some evidence against a tilted helix in thin bilayers from ionization experiments. The Asp residue for pLeu(D11) incorporated into di C18:1 vesicles ionizes with a pK_a of 8.6, consistent with a highly buried location. This pK_a is lower [close to pH 7, the value found COOH which are located at the membrane surface (Abrams et al., 1992)] both in thin (di C14:1 PC) and thick (di C24:1 PC/diC22:1 PC 2/1) model membranes, suggesting that in both thick and thin bilayers the Asp residues are located at the membrane surface (data not shown), whereas in a tilted helix the Asp would remain deeply buried. Nevertheless, we are uncertain of the structure of pLeu(D11) in the thin bilayers at this time.

Effect of Helix Length/Bilayer Width Ratio on Energetics of Transmembrane Orientation. To crudely estimate the energetic cost of having a hydrophobic sequence shorter than optimal for fully spanning the hydrophobic region of the bilayer (hydrophobic mismatch), the equilibrium between the transmembrane and nontransmembrane orientations was evaluated. The amount of each conformation present was roughly determined from the value of λ_{max}, and from these values the estimated free energy for transmembrane orientation (ΔG_{TM}) was calculated (see Theory). It should be emphasized that ΔG_{TM}, transmembrane free energy, is the difference in free energy for the transmembrane and lowest energy nontransmembrane, *but still membrane-associated*, conformation.

The partial dependence of $\Delta G_{TM}°$ on acyl chain length is shown in Figure 10A. The slope of $\Delta G_{TM}°$ in Figure 10A is equal to $\Delta\Delta G_{TM}°$, the change in free energy per change in bilayer width. From Figure 10A, $\Delta\Delta G_{TM}°$ is approximately 1−1.5 kcal/mol per two carbon increase in acyl chain length above 20 carbons.

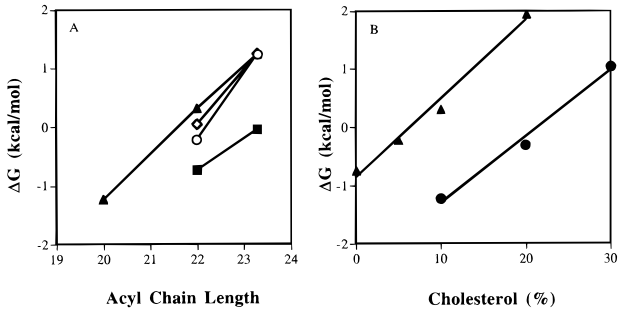

FIGURE 10: Effect of bilayer structure on stability of transmembrane orientation. (A) Effect of long acyl chain length on transmembrane stability under various conditions. Analysis of λ_{max} data was used to calculate $\Delta G_{TM}°$ (■) with different acyl chain width lipids; (○) different acyl chain length lipids plus 5% cholesterol; (▲) different acyl chain length lipids plus 10% cholesterol; (◇) different acyl chain length lipids plus 5 μL of 1:9 decane/ethanol. The lines shown are to illustrate the approximate average slope (=$\Delta\Delta G_{TM}°$) and *not* to imply a linear relationship of $\Delta G_{TM}°$ on acyl chain length. (B) Effect of cholesterol on transmembrane stability. Data from Figures 5 and 6 was used to calculate $\Delta G_{TM}°$ for (●) di C20:1 PC and (▲) di C22:1 PC with various amounts of cholesterol.

Since the change in acyl chain length is 0.9 Å per carbon atom (Chattopadhyay & London, 1987) (i.e., bilayer width changes 1.8 Å per carbon atom increase in acyl chain length) and the change in α-helix length is 1.5 Å per amino acid residue, $\Delta\Delta G_{TM}°$ would be about 0.5 kcal/mol on a per mismatched hydrophobic residue basis. Thus, the difference in transmembrane free energy between a 20 and 25 residue hydrophobic helix would be significant.

The energetic effect of cholesterol can also be calculated. The slope of the lines in Figure 10B shows that $\Delta\Delta G_{TM}°$ is about 1−1.5 kcal/mol/10% cholesterol for di C20:1 PC or di C22:1 PC. Thus, cholesterol concentration changes within a range observed *in vivo* (0−30%) are sufficient to strongly influence transmembrane insertion if the relationship between helix length and bilayer width is not optimal (see Discussion).

DISCUSSION

Helix Location Is Sensitive to Mismatch. Previous studies have shown that the ratio of bilayer width to hydrophobic helix length can have significant effects on membrane protein activity (Caffrey & Feigenson, 1981; Johannsson et al., 1981) and can result in the distortion of the bilayer to obtain a better match between bilayer width and helix length (see the introduction section). This study shows that bilayer distortion by itself can be insufficient to maintain stable transmembrane insertion even when a hydrophobic helix length differs only a few angstroms from the width of the hydrophobic segment of the bilayer. It is clear that when the bilayer width is longer than the helix, this mismatch results in a switch to a nontransmembrane orientation. We are less certain of the exact structure when the helix is longer than the width of the hydrophobic segment of the bilayer.

Potential Physiological Effects of Variations in Helix Length. Not every change in bilayer width alters helix orientation. In di C18:1 PC, pLeu(D11) helix orientation was unaffected by the addition of cholesterol or decane. Since di C18:1 PC is close to natural lipids in width, this implies that transmembrane helices with a hydrophobic stretch close to 20 residues can be stably inserted in a transmembrane form over a variety of naturally occurring bilayer widths.

Nevertheless, since transmembrane helices vary significantly in length [at least between 17 and 25 residues

(Henderson et al., 1990; Bretscher & Munro, 1993)], the bilayer width/helix length ratio should be a major influence on transmembrane orientation in other cases (Bretscher & Munro, 1993). In membrane proteins with extended polar flanking sequences on both sides of the membrane, an interconversion between transmembrane and nontransmembrane conformations is unlikely. In such cases, mismatch may be compensated for by helix tilting, helix−helix interactions and/or bilayer distortion. On the other hand, for helical hairpins (i.e., helix pairs) linked by short hydrophilic loops [such as in bacteriorhodopsin (Henderson et al., 1990)], mismatch of helix length and bilayer width could result in loss of transmembrane orientation. In any case, the loss of Ca^{2+}ATPase catalytic activity in thick and thin bilayers shows that mismatch can produce significant changes in membrane protein structure and function (Caffrey & Feigenson, 1981; Johannsson et al., 1981). In preliminary studies in collaboration with the lab of R. J. Collier (Harvard Medical School), we have also found that membrane thickness controls helix orientation for membrane inserted diphtheria toxin.

Potential Physiological Effects of Variations in Bilayer Thickness Due to Cholesterol. Cellular modulation of bilayer width by cholesterol may also have an influence on transmembrane orientation. Coupling of the modulation of bilayer width by cholesterol to helix length has been proposed as a mechanism of controlling membrane protein sorting based on the observation that membrane proteins in cholesterol-rich membranes (e.g., plasma membranes) have longer membrane-spanning sequences than those in membranes with less cholesterol (e.g., Golgi) (Bretscher & Munro, 1993). The present report demonstrates that the differences in cholesterol concentration in different membranes are sufficient to regulate transmembrane insertion. This could in turn affect the final membrane destination of a protein. For example, a transmembrane protein should partition best into membrane domains with optimal (matching) width. If a budding sorting vesicle had a different bilayer width than the other regions of the membrane, it could influence which transmembrane proteins enter the vesicle and travel to the target membrane (Munro, 1995).

Sequence Effects. We originally included the Asp residue in the helix to destabilize transmembrane insertion sufficiently to detect the nontransmembrane conformation. However, we have recently found the nontransmembrane conformation can be observed even if the Asp residue is not present (data not shown). It will be of interest in future studies to see how helix sequence alters transmembrane insertion and the response to changes in the helix length/bilayer width ratio.

REFERENCES

Abrams, F. S., & London, E. (1992) *Biochemistry 31*, 5312−5322.

Abrams, F. S., & London, E. (1993) *Biochemistry 32*, 10826−10831.

Abrams, F. S., Chattopadhyay, A., & London, E. (1992) *Biochemistry 32*, 5322−5327.

Asuncion-Punzalan. E. & London, E. (1995) *Biochemistry 34*, 15475−15479.

Batzri, S., & Korn, E. D. (1973) *Biochim. Biophys. Acta 298*, 1015−1019.

Bolen, E., & Holloway, P. (1990) *Biochemistry 29*, 9638−9643.

Bretscher, M. S., & Munro, S. (1993) *Science 261*, 1280−1281.

Caffrey, M., & Feigenson, G. W. (1981) *Biochemistry 20*, 1949−1961.

Cantor, C. R., & Schimmel, P. R., (1980) *Biophys. Chem. Biophysical Chemistry*, Part II, p 363, Freeman & Co., San Francisco.

Chattopadhyay, A., & London, E. (1987) *Biochemistry 26*, 39−45.

Chung, L. A., Lear, J. D., & DeGrado, W. F. (1992) *Biochemistry 31*, 6608−6616.

Davis, J. H., Clare, D. M., Hodges, R. S., & Bloom, M. (1983) *Biochemistry 22*, 5298−5305.

Haydon, D. A., Hendry, B. M., Levinson, S. R., & Requena, J. (1977) *Biochim. Biophys. Acta 470*, 17−34.

Henderson, R., Baldwin, J. M., Ceska, T. A., Zemlin, F., Beckmann, E., & Downing K. H. (1990) *J. Mol. Biol. 213*, 899−929.

Hope, M. J., Bally, M. B., Webb, G., & Cullis, P. R. (1985) *Biochim. Biophys. Acta 182*, 55−65.

Huschilt, J. C., Millman, B. M., & Davis, J. H. (1989) *Biochim. Biophys. Acta 979*, 139−141.

Johannsson, A., Keigthley, C. A., Smith G. A., Richards, C. D., Hesketh, T. R., & Metcalfe, J. C. (1981) *J. Biol. Chem. 256*, 1643−1650.

Kachel, K., Punzalan-Asuncion, E., & London, E. (1995) *Biochemistry 34*, 15475−15479.

Killian, J. A., Salemink, I., de Planque, M. R. R., Lindblom, G., Koeppe, R. E., II, & Greathouse, D. V. (1996) *Biochemistry 35*, 1037−1045.

Landolt-Marticorena, C., Williams, K. A., Deber, C. A., & Reithmeier, R. A. F. (1993) *J. Mol. Biol. 229*, 602−608.

Lew, S., & London, E. (1997) *Anal. Biochem.* (in press).

Lewis, B. A., & Engelman, D. M. (1983) *J. Mol. Biol. 166*, 211−217.

Mao, D., & Wallace, B. A. (1984) *Biochemistry 23*, 2667−2673.

Munro, S. (1995) *EMBO J. 14*, 4695−4704

Nezil, F. A., & Bloom, M. (1992) *Biophys. J. 61*, 1176−1183.

Sambrook, J., Fritsch, E. F., & Maniatis, T. (1989) *Molecular Cloning: A Laboratory Manual*, Cold Spring Harbor Press, Plainview, NY.

Sreerama, N., & Woody, R. W. (1993) *Anal. Biochem. 209*, 32−44.

Sreerama, N., & Woody, R. W. (1994) *Biochemistry 33*, 10022−10025.

Zhang, Y.-P., Lewis, R. N. A. H., Hodges, R. S., & McElhaney, R. N. (1992a) *Biochemistry 31*, 11572−11578.

Zhang, Y.-P., Lewis, R. N. A. H., Hodges, R. S., & McElhaney, R. N. (1992b) *Biochemistry 31*, 11579−11588.

BI9709295